Hedgehog inhibits β-catenin activity in synovial joint development and osteoarthritis

Jason S. Rockel,[1] Chunying Yu,[1] Heather Whetstone,[1] April M. Craft,[2] Katherine Reilly,[1] Henry Ma,[1] Hidetoshi Tsushima,[3] Vijitha Puviindran,[3] Mushriq Al-Jazrawe,[1] Gordon M. Keller,[2] and Benjamin A. Alman[1,3]

[1]Developmental and Stem Cell Biology, The Hospital for Sick Children, Toronto, Ontario, Canada. [2]McEwen Centre for Regenerative Medicine, University Health Network, Toronto, Ontario, Canada. [3]Department of Orthopaedic Surgery, Duke University, Durham, North Carolina, USA.

Both the WNT/β-catenin and hedgehog signaling pathways are important in the regulation of limb development, chondrocyte differentiation, and degeneration of articular cartilage in osteoarthritis (OA). It is not clear how these signaling pathways interact in interzone cell differentiation and synovial joint morphogenesis. Here, we determined that constitutive activation of hedgehog signaling specifically within interzone cells induces joint morphological changes by selectively inhibiting β-catenin–induced *Fgf18* expression. Stabilization of β-catenin or treatment with FGF18 rescued hedgehog-induced phenotypes. Hedgehog signaling induced expression of a dominant negative isoform of TCF7L2 (dnTCF7L2) in interzone progeny, which may account for the selective regulation of β-catenin target genes observed. Knockdown of TCF7L2 isoforms in mouse chondrocytes rescued hedgehog signaling–induced *Fgf18* downregulation, while overexpression of the human dnTCF7L2 orthologue (dnTCF4) in human chondrocytes promoted the expression of catabolic enzymes associated with OA. Similarly, expression of *dnTCF4* in human chondrocytes positively correlated with the aggrecanase *ADAMTS4*. Consistent with our developmental findings, activation of β-catenin also attenuated hedgehog-induced or surgically induced articular cartilage degeneration in mouse models of OA. Thus, our results demonstrate that hedgehog inhibits selective β-catenin target gene expression to direct interzone progeny fates and articular cartilage development and disease. Moreover, agents that increase β-catenin activity have the potential to therapeutically attenuate articular cartilage degeneration as part of OA.

Introduction

In the limbs, the growth plate provides the cartilage template that is turned over into bone during the process of endochondral ossification. Growth plate chondrocytes are responsible for bone growth during prenatal and postnatal development, a process regulated, in part, by Indian hedgehog–induced (IHH-induced) hedgehog signaling (1).

Synovial joints, composed of multiple tissue types, including synovium, menisci (in the knee), and articular cartilage, separate adjacent bones and function as sites of articulation. Articular cartilage caps the ends of bones, providing a low-friction surface for motion. Articular chondrocytes produce and maintain the extracellular matrix of articular cartilage, which forgoes the endochondral ossification process, persisting throughout adulthood. Superficial zone (SFZ) cells found at the surface of articular cartilage are the least chondrogenic of the articular chondrocytes and express lubricin, a proteoglycan responsible for maintaining joint integrity (2). In osteoarthritis (OA), a degenerative joint disease, articular cartilage is degraded and osteophytes (ectopic bone) are formed, in part, by increased hedgehog signaling in articular chondrocytes, mimicking the endochondral ossification process (3, 4). In addition, bone underlying the articular cartilage thickens, a response proposed to be a result of mechanical stress–induced TGF-β signaling in osteoblast precursors within the subchondral bone (5).

Synovial joint cells are derived from growth and differentiation factor 5–expressing (GDF5-expressing) interzone cells (6). Interzone cells first appear in the mouse forelimb between E11 and E11.5. During differentiation, interzone progenitor cells downregulate the expression of chondrogenic markers COL2A1 and SOX9 and instead express GDF5 (7, 8). Interzone cells then differentiate into synovial joint cells, including articular chondrocytes, but do not contribute to growth plate chondrocytes. The signaling mechanisms responsible for the differentiation of interzone progeny, including chondrocytes, are not well understood.

Interzone differentiation is dependent on multiple pathways, including canonical WNT and hedgehog (9–12). Activation of hedgehog signaling prior to interzone formation induces joint fusions through increased BMP expression (1, 12). In contrast, *Ihh*-deficient mice fail to form joints in the distal hind limbs (13). This suggests that joint morphogenesis is, in part, dependent on spatial regulation of hedgehog signaling. WNT ligand–induced β-catenin activity is necessary for joint formation and maintenance (9, 10, 14). Hedgehog and canonical WNT signaling interact to regulate cell fates in a variety of other developmental contexts (15–17); however, it is unclear how hedgehog and canonical WNT signaling interact in interzone cells.

Note regarding evaluation of this manuscript: Manuscripts authored by scientists associated with Duke University, The University of North Carolina at Chapel Hill, Duke-NUS, and the Sanford-Burnham Medical Research Institute are handled not by members of the editorial board but rather by the science editors, who consult with selected external editors and reviewers.

Conflict of interest: The authors have declared that no conflict of interest exists.

Submitted: November 25, 2014; **Accepted:** February 11, 2016.

Reference information: *J Clin Invest*. 2016;126(5):1649–1663. doi:10.1172/JCI80205.

We sought to determine how hedgehog and WNT/β-catenin signaling interact to regulate interzone cells and their progeny and found that hedgehog signaling regulation is necessary for appropriate joint morphogenesis. Hedgehog signaling inhibited selective β-catenin target gene expression, including that of *Fgf18*, but did not change β-catenin localization in vivo. Rather, hedgehog induced the expression of dominant negative TCF7L2 (dnTCF7L2), which was partially responsible for the reduction in *Fgf18* expression. Phenotypes associated with hedgehog activation could be rescued by β-catenin modulation or exogenous FGF18. Our findings show a link between hedgehog and β-catenin–induced FGF18 expression in interzone progeny and also show how this signaling balance modulates tissue morphogenesis. Furthermore, we found that the balance of hedgehog and β-catenin signaling is critical to the maintenance of articular cartilage in adult mouse models of OA and that expression of the dnTCF7L2 orthologue, dnTCF4, in human chondrocytes likely plays a role in cartilage degeneration via regulating expression of ADAMTS4. Thus, factors that modulate β-catenin activity may be beneficial in the therapeutic treatment of OA.

Results

Regulation of hedgehog signaling in interzone cells is necessary for joint and long bone morphogenesis. To determine the effect of hedgehog signaling on joint morphogenesis and skeletal development, we studied embryonic development in mice that had constitutively active or inactive hedgehog signaling in interzone-derived cells (Figure 1 and Supplemental Figures 1–3; supplemental material available online with this article; doi:10.1172/JCI80205DS1). Unexpectedly, we found that *Smo$^{fl/fl}$ Gdf5-Cre* mice did not show any overt skeletal phenotype during development up until birth (Supplemental Figure 1). Interestingly, however, we found that mice that had activated hedgehog signaling in interzone progeny (*Ptch1$^{fl/fl}$ Gdf5-Cre* and *SmoM2$^{fl/+}$ Gdf5-Cre* mice, where *Ptch1* indicates patched 1) were perinatal lethal. *Ptch1$^{fl/fl}$ Gdf5-Cre* and *SmoM2$^{fl/+}$ Gdf5-Cre* P0 mice had ossified rib cages, shorter ossified regions in the long bones, elongated cartilaginous regions at the ends of the bones, and irregular bone collars at the cartilage-bone interface compared with Cre$^-$ mice (Figure 1, A–C, F–H, K–M, and Supplemental Figure 2, A–C, F, and G). At P0 and E17.5, these mice had morphological changes in the knee joint, including loss of menisci and ectopic cartilage protruding from the proximal tibia (Figure 1, F–H, K–M, and P–R), longer tibial growth plates due to an expansion of the proliferative zone, and longer bone collars surrounding the growth plates as compared with Cre$^-$ controls (Figure 1, U–W, Z–BB, and Supplemental Figure 2, H–K). Although the length of the domain occupied by type X collagen matrix was not altered in growth plates of mice with active hedgehog signaling (*SmoM2$^{fl/+}$ Gdf5-Cre)* compared with Cre$^-$ growth plates, there was a reduced number of cells occupying the zone of type X collagen deposition (Supplemental Figure 3, A, B, E, and F), suggesting a delay in growth plate chondrocyte maturation and differentiation. Thus, hedgehog signaling in interzone cells has primary effects on joint morphology and secondary effects on growth plate and bone development.

Hedgehog signaling regulates interzone cell fate and joint morphogenesis. We next determined the effect of hedgehog signaling in interzone cells on chondrocyte differentiation. We used *R26RLacZ$^{fl/fl}$ Gdf5-Cre* mice to track the differentiation of interzone progeny into chondrocytes at the surface of the tibia. Fate map analysis using X-gal–stained *R26RLacZ$^{fl/fl}$ Gdf5-Cre* hind limb sections showed that synovial joint cells, but not underlying growth plate chondrocytes, were derived from *Gdf5*-expressing progenitor cells, consistent with previous results (Figure 2, A and E, and ref. 6). Fate map analysis of E17.5 mice with active hedgehog signaling (*R26RLacZ$^{fl/+}$ SmoM2$^{fl/+}$ Gdf5-Cre* mice) identified the cells filling the joint space as well as the ectopic tibial cartilage (as described above; Figure 1, Q and R) as being derived from *Gdf5*-expressing progenitors by X-gal staining (Figure 2B). However, we found that the area of X-gal–positive chondrocytes within the tibial surface cartilage, defined by cells within the proteoglycan-rich (safranin O [SafO] stained) region, was reduced in *R26RLacZ$^{fl/+}$ SmoM2$^{fl/+}$ Gdf5-Cre* mice compared with *R26RLacZ$^{fl/fl}$ Gdf5-Cre* control mice (Figure 2, C–G). Thus, hedgehog signaling inhibits interzone cell differentiation to chondrocytes at the tibial surface.

To identify the phenotype of the cells occupying the knee-joint space in mice with active hedgehog signaling (*SmoM2$^{fl/+}$ Gdf5-Cre*), we performed in situ hybridizations for markers of chondrocytes and osteoblasts in E17.5 hind limb sections. In addition to expressing *Ptch1* and parathyroid hormone-like hormone (*Pthlh*), readouts for activation of hedgehog signaling in this cell population (Supplemental Figure 4, A, B, E, and F), these cells did not express chondrocyte markers sex determining region Y–box 9 (*Sox9*) or collagen type II alpha 1 (*Col2a1*) (Figure 2, H–K), nor was there mineralized tissue (data not shown). However, the cells did express a low level of *Col1a1*, consistent with a mesenchymal phenotype (Figure 2, L and M). We also found that the proliferation marker Ki67 was expressed in this population of cells, which was absent from Cre$^-$ controls (Figure 2, N and O); these data are consistent with these cells being a proliferating, mesenchymal-like population.

Hedgehog signaling inhibits β-catenin target gene expression in interzone progeny. At E14.5, mice did not have ectopic cartilage in the tibia in any of the transgenic lines studied (Figure 3, A–D). Lineage tracing of interzone progeny using *R26RLacZ$^{fl/fl}$ Gdf5-Cre* mice at E14.5 showed that the loosely packed population of cells bordered by cartilage, ligaments, and tendons was derived from interzone progeny (Figure 3E). This population of cells demonstrated a less-differentiated phenotype than other interzone-derived cells in tissues surrounding it, including cartilage, as defined by SafO staining, and ligament/tendon, as defined by stacked cells oriented in parallel (Figure 3, A–D). To determine how hedgehog and WNT/β-catenin signaling might interact in this, and possibly other interzone-derived progeny, we used in situ hybridization to determine changes in the expression pattern of select β-catenin target genes (Figure 3, F–O). The number of cells expressing *Fgf18*, a tissue-selective β-catenin target gene expressed by interzone progeny (18–20), was reduced in mice with active hedgehog signaling (*SmoM2$^{fl/+}$ Gdf5-Cre* mice) as compared with Cre$^-$ mice, while the number of cells expressing *Axin2* did not change (Figure 3, F, G, J, K, L, and O).

We next determined whether β-catenin localization was altered in vivo in response to hedgehog activation. There was no significant difference in the percentage of interzone progeny with nuclear

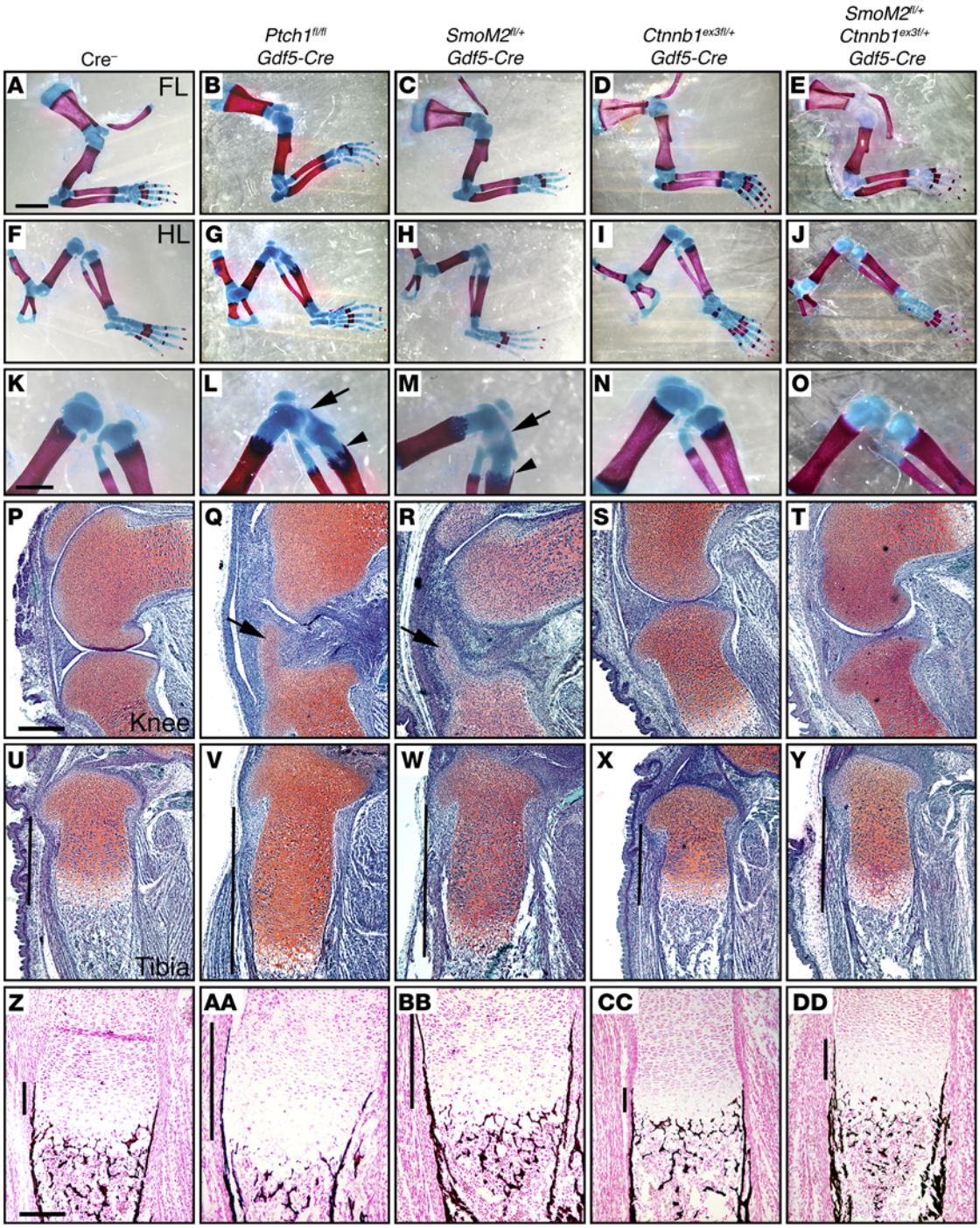

Figure 1. Hedgehog signaling in interzone cells results in morphological changes to the joint and osteochondrodysplasias of the long bones that can be rescued by activation of β-catenin. Mice were collected at P0 (**A**–**O**) or E17.5 (**P**-**DD**). (**A**–**O**) Skeletons were stained by Alcian blue/Alizarin red to identify cartilage/bone. FL, forelimb; HL, hind limb. (**P**–**Y**) Histological hind limb sections stained with SafO to identify cartilage (orange). (**U**–**Y**) Black bars indicate growth plate length. (**Z**-**DD**) Histological sections of hind limbs stained with von Kossa to identify bone (black/brown). Black bars indicate length of bone collar around the growth plate. (**L** and **M**) Arrowheads indicate extended bone collar surrounding the growth plate. (**L**, **M**, **Q**, and **R**) Arrows indicate ectopic cartilage. (**A**–**DD**) Images are representative of $n \geq 4$ for all genotypes. Scale bars: 1 mm (**A**); 2 mm (**K**); 200 μm (**P**); 100 μm (**Z**). See also Supplemental Figures 1–3.

localization of β-catenin by immunohistochemistry in hedgehog active (*SmoM2$^{fl/+}$ Gdf5-Cre*) mice compared with Cre$^-$ mice (Figure 3, P and Q; Cre-: 20.06% ± 2.263% vs. *SmoM2$^{fl/+}$ Gdf5-Cre*: 19.67% ± 1.867%; mean ± SEM, $P > 0.05$ by Student's *t* test, $n = 5$ per genotype). The observed inhibition of β-catenin target gene expression without changes in β-catenin localization raised the possibility that a negative transcriptional regulator of β-catenin target genes was affecting expression. Hedgehog activity in the dorsal retina of mice induced the expression of dnTCF7L2 (16), whose full-length form is known to complex with β-catenin and is required for the expres-

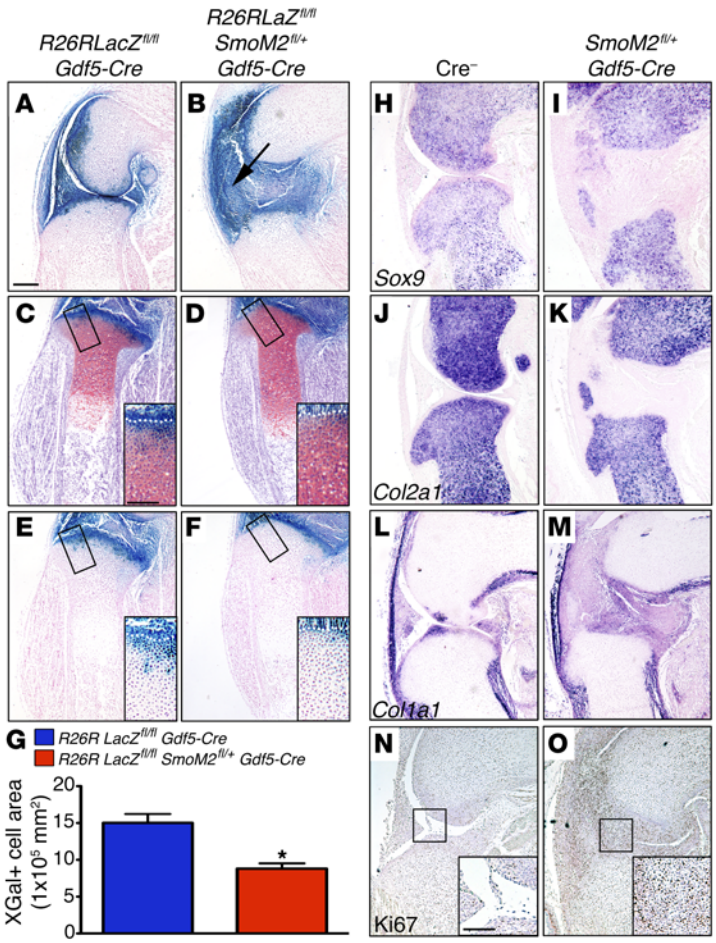

Figure 2. Hedgehog signaling inhibits differentiation of interzone progeny into articular chondrocytes. (**A**–**F**) Hind limb sections from the medial (**A** and **B**) or central (**C**–**F**) knee stained with X-gal/Nuclear Fast Red (**A**, **B**, **E**, and **F**) or X-gal/SafO (**C** and **D**) of E17.5 *R26RLacZ*$^{fl/fl}$ *Gdf5-Cre* (**A**, **C**, and **E**) and *R26RLacZ*$^{fl/+}$ *SmoM2*$^{fl/+}$ *Gdf5-Cre* (**B**, **D**, and **F**) mice. (**B**) Arrow indicates ectopic cartilage. (**C**–**F**) Insets show reduced depth of X-gal–stained cells in the cartilage (SafO-stained region) in *R26RLacZ*$^{fl/+}$ *SmoM2*$^{fl/+}$ *Gdf5-Cre* mice compared with *R26RLacZ*$^{fl/fl}$ *Gdf5-Cre* mice, as marked by the white dotted line. (**G**) The area of X-gal$^+$ cells as part of the tibial plateau in the center of the joint was measured and analyzed by Student's *t* test. Bars indicate mean ± SEM. $^*P < 0.01$, $n \geq 4$ per genotype. (**H**–**Q**) E17.5 Cre$^-$ and *SmoM2*$^{fl/+}$ *Gdf5-Cre* hind limbs were sectioned and stained by in situ hybridization for *Sox9* (**H** and **I**), *Col2a1* (**J** and **K**), and *Col1a1* (**L** and **M**), or by immunohistochemistry for Ki67 as a marker of proliferation (**N** and **O**). (**N** and **O**) Inset shows expression of Ki67$^+$ cells occupying the joint space in *SmoM2*$^{fl/+}$ *Gdf5-Cre* embryonic knees (**O**) compared with an absence of proliferating cells in Cre$^-$ mice (**N**). (**H**–**O**) Images are representative of $n \geq 3$. Scale bars: 200 μm (**A**); 100 μm (**C** and **N**, insets). See also Supplemental Figure 4.

sion of *Fgf18* (18, 19). Hedgehog active mice (*SmoM2*$^{fl/+}$ *Gdf5-Cre*) had a significantly increased number of interzone-derived cells expressing *dnTcf7l2* as compared with Cre$^-$ mice (Figure 3, R–T). Collectively, these data suggest that selective β-catenin target gene expression is inhibited by hedgehog signaling in interzone progeny, likely through expression of TCR isoforms such as dnTCF7L2.

Isoforms of TCF7L2/TCF4 regulate the expression of Fgf18 and target genes associated with cartilage destruction in OA in mouse and human chondrocytes. Primary costal chondrocytes isolated from C57BL/6 mice were used to determine the contribution of isoforms of TCF7L2 to the expression of FGF18. Primary chondrocytes were treated with purmorphamine (PM) and transfected with siRNA to reduce the expression of TCF7L2 isoforms. PM treatment increased the protein levels of both full-length and dominant negative isoforms of TCF7L2, while transfection of siRNA against all isoforms of TCF7L2 reduced the PM-induced expression of all isoforms of TCF7L2 (Figure 4A). siRNA knockdown of TCF7L2 isoforms rescued reductions in *Fgf18* RNA expression induced by PM without significantly affecting the expression of *Axin2* or the hedgehog target gene *Gli1* (Figure 4, B–D).

Primary mouse SFZ cells, the least chondrogenic progeny of the interzone as part of articular cartilage, have vastly different gene-expression profiles as compared with the remaining articular chondrocytes, including higher expression levels of *Fgf18* (21). Similar to our findings in costal chondrocytes, treatment of isolated SFZ cells with PM in vitro significantly reduced *Fgf18* but not *Axin2* RNA levels; however, PM treatment significantly reduced both WNT3a-induced *Axin2* and *Fgf18* RNA levels (Supplemental Figure 4, J and K). In addition, the ratio of RNA expression of a dn*Tcf7l2* isoform to full-length *Tcf7l2* was increased (Supplemental Figure 4L), suggesting a shift toward *dnTcf7l2* expression.

We next evaluated the effect of a dominant negative human orthologue of TCR7L2, dnTCF4, on the expression of β-catenin target genes and markers of cartilage degradation in human chondrocytes (Figure 4, E–K). Primary human chondrocytes isolated from femoral condyles of knees from patients undergoing knee-replacement surgery were cultured and infected with adenovirus to express dnTCF4 or GFP (as a control). Chondrocytes infected with the dnTCF4-expressing adenovirus vector had significantly increased levels of dnTCF4 protein and total *TCF4* transcripts compared with cells infected with GFP adenovirus (Figure 4, E and F). As anticipated, dnTCF4-infected cells had reduced levels of the β-catenin target genes *AXIN2* and *FGF18* (Figure 4, G and H). Interestingly, however, these cells also had significant increases in the RNA expression of *MMP13*, *MMP3*, and *ADAMTS4* (Figure 4, I–K), genes whose protein products mediate the destruction of extracellular matrix components of cartilage (22–25). Overall, these data are consistent with the notion that TCF7L2/TCF4 isoforms, including dominant negative isoforms, play a critical role in regulating β-catenin target genes downstream of hedgehog sig-

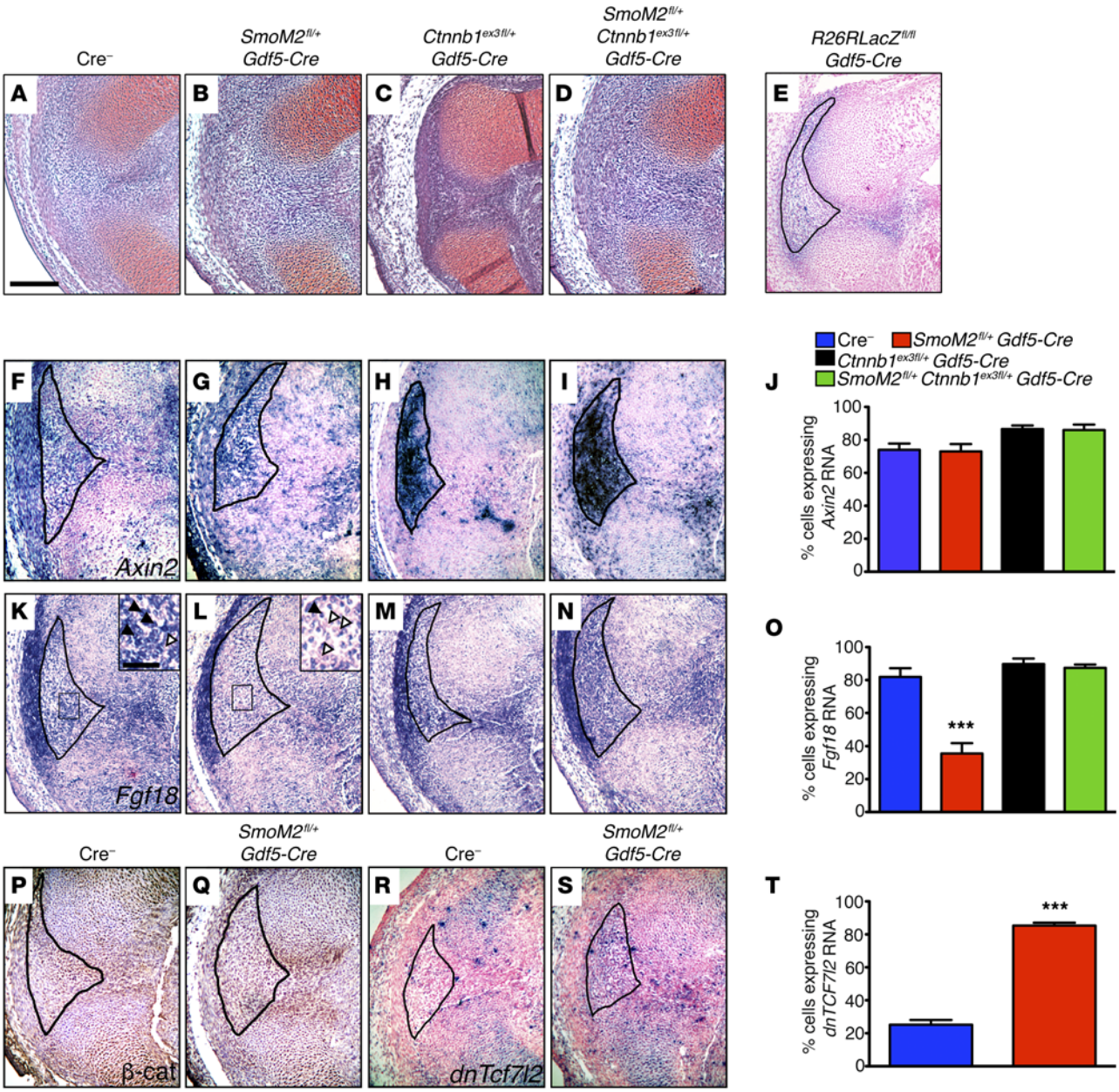

Figure 3. Hedgehog signaling inhibits selected β-catenin target gene expression in interzone progeny. E14.5 hind limb sections were stained for SafO (**A**–**D**), X-gal (**E**), *Axin2* (**F**–**I**), *Fgf18* (**K**–**N**), *Ctnnb1* (**P** and **Q**), or *dnTcf7l2* (R & **S**) by histochemistry (**A**–**E**), in situ hybridization (**F**–**N**, **R**, and **S**), or immunohistochemistry (**P** and **Q**). Images are representative of $n \geq 3$ embryos per genotype. Traced areas represent the interzone-derived progeny, as indicated by lineage tracing (**E**). Cells expressing *Axin2*, *Fgf18*, and *dnTcf7l2* were counted (**J**, **O**, and **T**). (**J**, **O**, and **T**) Bars represent mean ± SEM. Data were analyzed by 1-way ANOVA followed by Tukey's post-hoc test (**O**) or Student's *t* test (**T**). ***$P < 0.001$ compared with all other bars. $n = 3$–4 per genotype. (**K** and **L** insets) Black arrowheads, *Fgf18*-positive cells; white arrowheads, *Fgf18*-negative cells. Scale bars: 200 μm (**A**); 50 μm (**K**, inset). See also Supplemental Figure 4.

naling and may also play a crucial role in regulating the expression of catabolic enzymes that are important in the breakdown of articular cartilage in OA.

β-Catenin activation attenuates phenotypes induced by hedgehog signaling modulation in part through regulating Fgf18 expression. Since our data suggested that hedgehog signaling was interfering with β-catenin–induced gene expression, we next determined whether we could rescue hedgehog-induced phenotypes by enhancing β-catenin activity through constitutive activation of β-catenin in vivo. We generated *SmoM2$^{fl/+}$ Ctnnb1$^{ex3fl/+}$ Gdf5-Cre* mice, which have constitutive activation of both hedgehog and β-catenin in *Gdf5*-expressing interzone progeny. The skeletons of mice with activated β-catenin alone in interzone progeny (*Ctnnb1$^{ex3fl/+}$ Gdf5-Cre*) were not overtly different compared with those of Cre⁻ mice at P0 (Supplemental Figure 2, A and D). At E17.5 and P0, there was no significant difference in the length of bone, cartilage, or zone of type X collagen deposition or cell density within the type X collagen zone in forelimbs, hind limbs, or tibias compared with Cre⁻ mice, except for the proximal cartilage of the ulna, which was shorter at P0 (Figure 1, A, D, F,

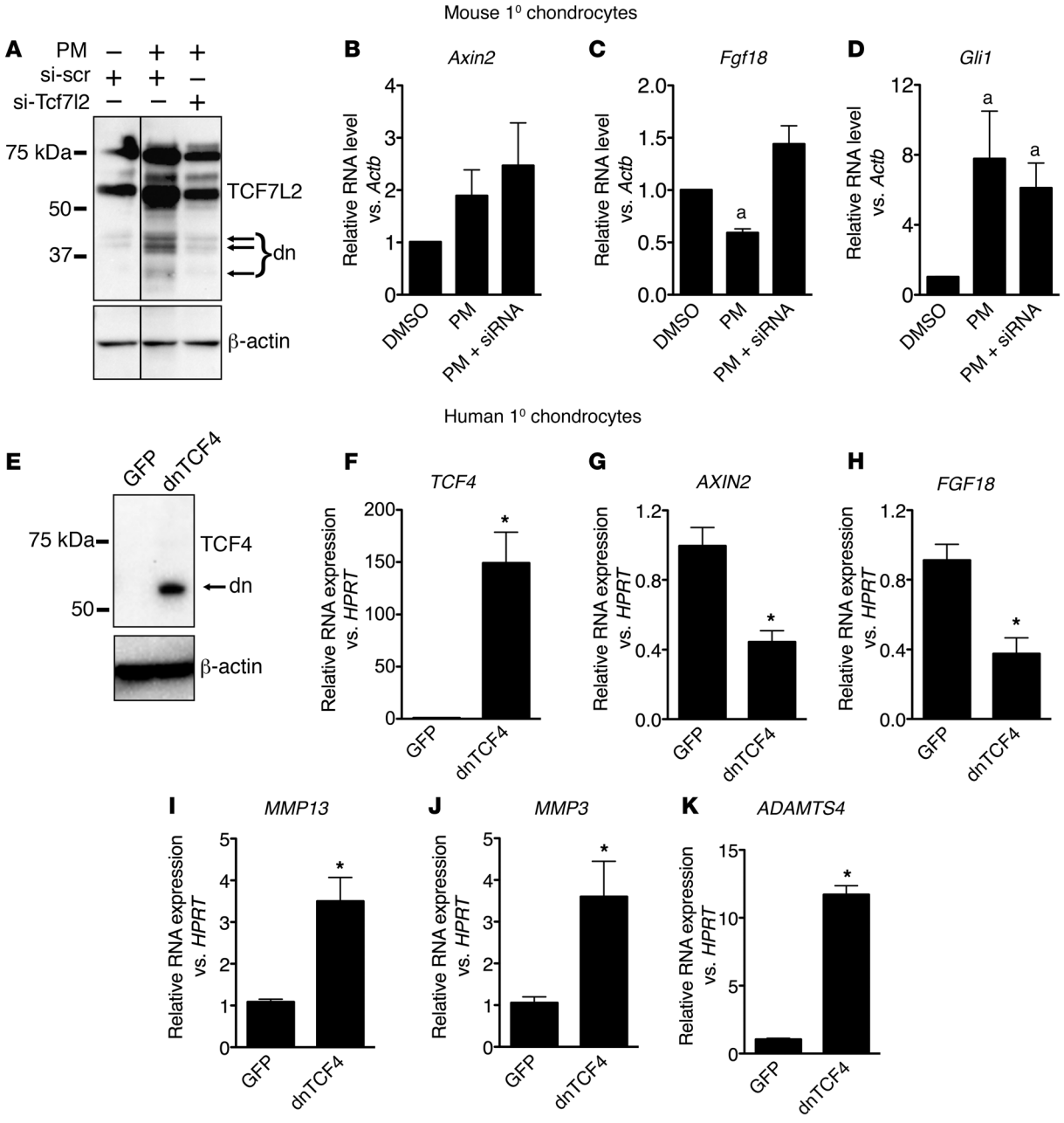

Figure 4. TCF isoforms regulate the expression of β-catenin target genes and markers of cartilage degeneration in mouse and human chondrocytes in vitro. Primary mouse costal chondrocytes (**A**–**D**) or human knee chondrocytes (**E**–**K**) were isolated and cultured. Protein levels of TCF7L2/TCF4 isoforms were determined by immunoblotting (**A** and **E**), and RNA levels of *Axin2* (**B** and **G**), *Fgf18* (**C** and **H**), *Gli1* (**D**), total *TCF4* (**F**), *MMP13* (**I**), *MMP3* (**J**), and *ADAMTS4* (**K**) were determined by qPCR relative to *Actb* (**B**–**D**) or *HPRT* (**F**–**K**). (**A**–**D**) Primary mouse chondrocytes were transfected with scrambled (DMSO or PM) or siRNA mix (PM + siRNA) that selectively targets all isoforms of *Tcf7l2* and treated with DMSO or PM (10 μM) for 48 hours. (**B**–**D**) Bars represent mean ± SEM normalized to DMSO-treated cultures. Data were log transformed prior to analysis by repeated-measures ANOVA followed by Tukey's post-hoc tests. a, significantly different ($P < 0.05$) compared with unlabeled bars. (**E**–**K**) Primary human chondrocytes were isolated and infected with adenoviral vectors expressing GFP or a dominant negative form of TCF4. (**E**–**K**) Bars represent mean ± SEM. Data were log transformed prior to analysis by paired *t* test. *$P < 0.05$ compared with GFP-infected cells. See also Supplemental Figure 4.

I, K, N, P, S, U, X, Z, and CC; Supplemental Figure 2, G, I, and K; and Supplemental Figure 3, A, C, E, and F). Compared with mice with active hedgehog signaling alone (*SmoM2$^{fl/+}$ Gdf5-Cre* or *Ptch1$^{fl/fl}$ Gdf5-Cre* mice), we found that mice that had both hedgehog and β-catenin active in interzone progeny (*SmoM2$^{fl/+}$ Ctnnb1$^{ex3fl/+}$ Gdf5-Cre* mice) also had ossified rib cages and were perinatal lethal; however, they did not form ectopic cartilage, had a significant reduction in tibial bone collar length, had significantly shorter tibial growth plates, and had significantly increased cell density in the type X collagen positive–zone of the growth plate, equivalent to that of Cre$^-$ and *Ctnnb1$^{ex3fl/+}$ Gdf5-Cre* mice (Figure 1 and Supplemental Figures 2 and 3). To verify that *Ctnnb1$^{ex3fl/+}$ Gdf5-Cre* mice regulated β-catenin target genes, we determined that *Ctnnb1$^{ex3fl/+}$ Gdf5-Cre* and *SmoM2$^{fl/+}$ Ctnnb1$^{ex3fl/+}$*

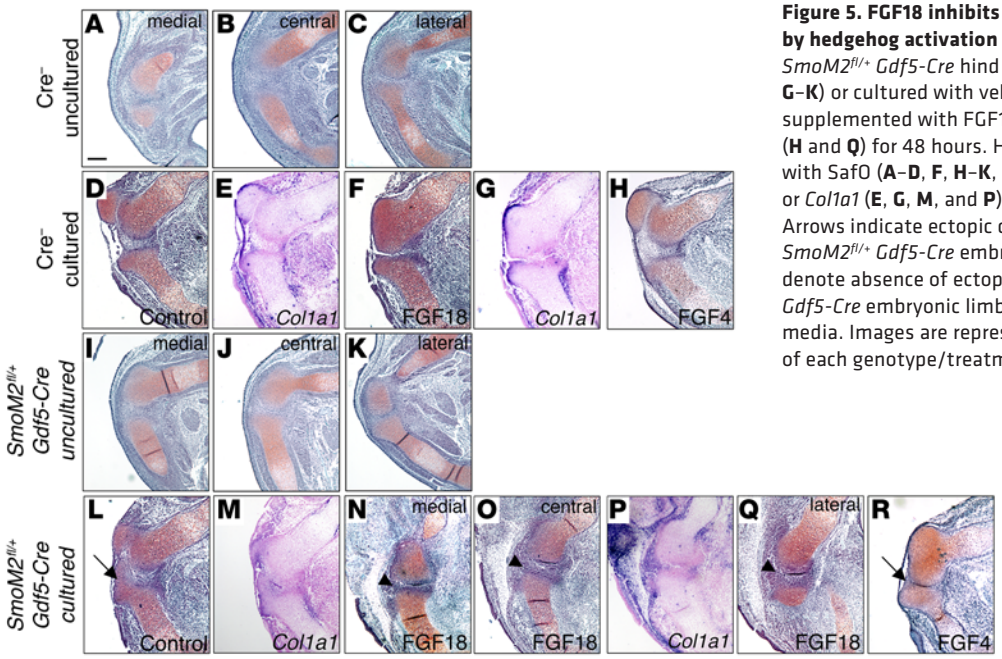

Figure 5. FGF18 inhibits ectopic cartilage formation induced by hedgehog activation in interzone progeny. E14.5 Cre⁻ and *SmoM2*$^{fl/+}$ *Gdf5-Cre* hind limbs were uncultured (**A**–**C** and **G**–**K**) or cultured with vehicle control (**D**, **E**, **L**, and **M**) or media supplemented with FGF18 (200 ng/ml; **F**, **G**, and **N**–**Q**) or FGF4 (**H** and **Q**) for 48 hours. Hind limbs were sectioned and stained with SafO (**A**–**D**, **F**, **H**–**K**, **L**, **N**, **O**, **Q**, and **R**) by histochemistry or *Col1a1* (**E**, **G**, **M**, and **P**) by in situ hybridization. (**L** and **R**) Arrows indicate ectopic cartilage formed on the tibia of a *SmoM2*$^{fl/+}$ *Gdf5-Cre* embryonic limb. (**N**, **O**, and **Q**) Arrowheads denote absence of ectopic cartilage on the tibia of *SmoM2*$^{fl/+}$ *Gdf5-Cre* embryonic limbs cultured in FGF18-supplemented media. Images are representative of $n \geq 3$ hind limb cultures of each genotype/treatment. Scale bar: 200 μm (**A**).

Gdf5-Cre mice had qualitatively stronger expression of *Axin2* compared with Cre⁻ or *Gdf5-Cre* and *SmoM2*$^{fl/+}$ *Gdf5-Cre* mice, but with a similar number of cells expressing *Axin2* (Figure 3, F–J). As compared with mice with active hedgehog signaling in interzone progeny (*SmoM2*$^{fl/+}$ *Gdf5-Cre* mice), mice with both active hedgehog and β-catenin (*SmoM2*$^{fl/+}$ *Ctnnb1*$^{ex3fl/+}$ *Gdf5-Cre*) had a significantly greater number of cells expressing *Fgf18* and a similar number compared with mice with active β-catenin alone (*Ctnnb1*$^{ex3fl/+}$ *Gdf5-Cre*) or Cre⁻ mice (Figure 3, K–O). Activation of β-catenin did not affect hedgehog-induced *Ptch1* or *Pthlh* expression by in situ hybridization in vivo or PM-induced *Ptch1* expression in SFZ cells by quantitative PCR (qPCR) in vitro (Supplemental Figure 4, A–I). Thus, hedgehog-induced interzone morphological changes are rescued by constitutive activation of β-catenin, suggesting that a threshold level of β-catenin activity is necessary to sustain the expression of *Fgf18*, possibly by competing with hedgehog-induced dnTCF7L2 for TCF-binding sites as a complex of β-catenin and full-length TCF isoforms (26).

To determine the contribution of FGF18 to the maintenance of joint morphogenesis, we cultured E14.5 hind limbs from Cre⁻ and hedgehog active mice (*SmoM2*$^{fl/+}$ *Gdf5-Cre*) in media containing recombinant FGF18 or FGF4 (as a control; Figure 5). Uncultured limbs from E14.5 *SmoM2*$^{fl/+}$ *Gdf5-Cre* mice did not have ectopic cartilage, consistent with Cre⁻ hind limbs (Figure 5, A–C, and I–K). We found no differences in hind limb morphology or localization of *Col1a1* expression after 48 hours of culture among control, FGF18-, or FGF4-treated Cre⁻ hind limbs (Figure 5, D–H). Cultured *SmoM2*$^{fl/+}$ *Gdf5-Cre* hind limbs formed ectopic cartilage on the tibia after 48 hours in culture in control media and contained cells expressing *Col1a1* within the presumptive joint space (Figure 5, L and M). *SmoM2*$^{fl/+}$ *Gd5-Cre* hind limbs cultured in FGF18-supplemented media did not form ectopic cartilage, but continued to have cells filling the presumptive joint space, which expressed *Col1a1* (Figure 5, N–Q). In contrast, ectopic cartilage was formed on the tibia in *SmoM2*$^{fl/+}$ *Gd5-Cre* hind limbs that were cultured with FGF4 (Figure 5R). These data support the notion that β-catenin–induced FGF18 expression prevents ectopic cartilage formation on the tibia and may be key in regulating joint cell differentiation and maintenance.

Activation of β-catenin can attenuate hedgehog and surgically induced articular cartilage degeneration. Hedgehog signaling is activated in articular chondrocytes during joint degeneration (4). We sought to determine whether β-catenin could attenuate hedgehog-induced joint degeneration in postnatal mice, similar to the rescue of joint morphogenesis seen in our developmental models. To evaluate the efficiency of tamoxifen-induced, *Col2-CreERT2*–mediated recombination, we generated *R26RLacZ*$^{fl/+}$ *Col2-CreERT2* mice. Six weeks after tamoxifen injection, 24.18% ± 5.31% (mean ± SE, $n = 4$) of the articular chondrocytes on the tibial surface of mouse knee joints showed evidence of recombination, as determined by X-gal staining (Supplemental Figure 5A). The majority of X-gal–stained cells were localized to the superficial and midzone chondrocytes, suggesting that these cells were most prone to *Col2-CreERT2*–induced recombination in articular chondrocytes of adult mice.

We focused on cartilage in the medial tibial plateau of mice, as our previous experience and that of others has shown this domain to be most prone to cartilage degeneration as a result of both spontaneous and surgically induced OA (27). We first activated hedgehog signaling in chondrocytes of mature mice that contained a tamoxifen-inducible *Col2-Cre* transgene (*SmoM2*$^{fl/+}$ *Col2-CreERT2*). Consistent with previous results (4), 6 weeks after tamoxifen injection, these mice had degenerative zones in the medial tibial articular cartilage compared with Cre⁻ controls. Mice with active hedgehog signaling (*SmoM2*$^{fl/+}$ *Col2-CreERT2*) had loss of proteoglycans, indicated by reduced SafO staining of the cartilage, evidence of vertical clefts, and loss of surface lamina, as determined histologically and quantified using OARSI scoring recommended for mouse

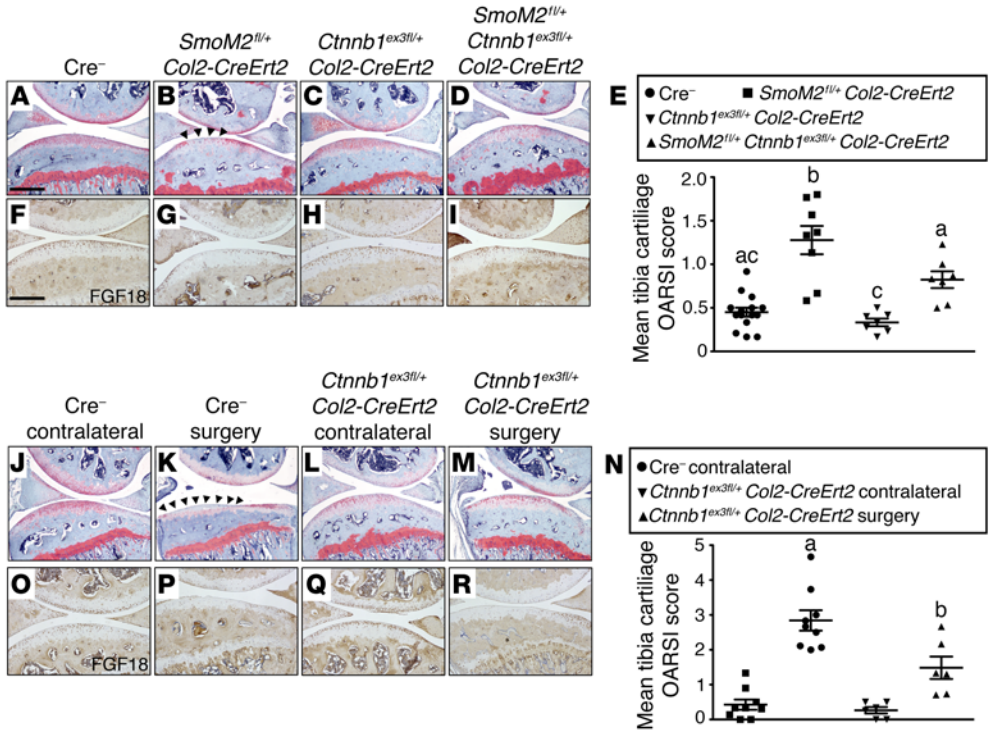

Figure 6. Activation of β-catenin in chondrocytes attenuates hedgehog and surgically induced articular cartilage degeneration. (**A**–**D** and **F**–**I**) Mice were injected with tamoxifen at 8 weeks of age. Hind limbs were collected after 6 weeks and stained with SafO (**A**–**D**) or for FGF18 by immunohistochemistry (**F**–**I**). (**J**–**R**) The medial meniscus of the left knee was surgically removed in 8-week-old mice. Tamoxifen was injected 6 days after surgery, and mice were collected at 7 weeks after surgery. Hind limbs sections were stained with SafO (**J**–**M**) or for FGF18 by immunohistochemistry (**O**–**R**). (**B** and **K**) Black arrowheads indicate zones of cartilage degeneration along the tibial surface. (**E** and **N**) Cartilage degeneration severity was graded by OARSI scoring recommended for the mouse. Individual points are an average of 3–8 sections from 2-4 slides separated by a minimum of 60 μm and graded by 3 blinded, independent reviewers. Bars represent mean ± SEM. Data were analyzed by 1-way ANOVA followed by Tukey's post-hoc tests. Unlabeled bars or bars labeled with the same letter are not significantly different from each other ($P > 0.05$). $n \geq 6$ animals per group. Scale bars: 400 μm (**A**); 200 μm (**F**). See also Supplemental Figures 5 and 6 and Supplemental Table 1.

models of OA (Figure 6, A, B, E, and ref. 28). In contrast, mice that had activation of both hedgehog and β-catenin in chondrocytes (*SmoM2$^{fl/+}$ Ctnnb1$^{ex3fl/+}$ Col2-CreERT2*) had reduced proteoglycan (SafO) staining. OARSI scoring of the medial tibial cartilage indicated that *SmoM2$^{fl/+}$ Ctnnb1$^{ex3fl/+}$ Col2-CreERT2* mice had significantly reduced medial tibial cartilage destruction compared with *SmoM2$^{fl/+}$ Col2-CreERT2* mice, with OARSI scores similar to those of mice with β-catenin signaling alone (*Ctnnb1$^{ex3fl/+}$ Col2-CreERT2*) or Cre$^-$ mice (Figure 6, A–E). No significant differences in subchondral bone thickness were seen between the genotypes (Supplemental Figure 6A). In addition, a significant increase in synovitis was seen in *SmoM2$^{fl/+}$ Col2-CreERT2* mice compared with Cre$^-$ mice or *Ctnnb1$^{ex3fl/+}$ Col2-CreERT2* mice. There was a moderate, but not significant, reduction in synovitis score in *SmoM2$^{fl/+}$ Ctnnb1$^{ex3fl/+}$ Col2-CreERT2* mice (Supplemental Figure 6C). Finally, in *SmoM2$^{fl/+}$ Col2-CreERT2* mice, we qualitatively observed cellular changes in the cartilage that were consistent with OA, including loss of SFZ cells, empty lacunae (indicative of cell death), reduced overall cellularity, and evidence of chondrocyte clusters. These cellular phenotypes were qualitatively reduced in *SmoM2$^{fl/+}$ Ctnnb1$^{ex3fl/+}$ Col2-CreERT2* mice (Supplemental Table 1).

We next wanted to determine whether joint degeneration due to mechanical injury could be attenuated by activation of β-catenin. We surgically removed the medial meniscus from the left hind limbs of Cre$^-$ mice or mice with conditional, tamoxifen-inducible β-catenin (*Ctnnb1$^{ex3fl/+}$ Col2-CreERT2*). Tamoxifen was administered 1 week after surgery. Six weeks after tamoxifen injection, the medial tibia of the surgical knee of Cre$^-$ mice showed significant tibial cartilage degeneration as compared with contralateral limbs, evidenced by vertical clefts and cartilage erosion covering approximately 25% of the cartilage surface, as determined by OARSI scoring (Figure 6, J, K, and N). Consistent with our hedgehog-induced joint degeneration model, *Ctnnb1$^{ex3fl/+}$ Col2-CreERT2* mice had significantly reduced joint degeneration as compared with Cre$^-$ mice, evidenced by a reduction of severe erosion or vertical clefts and quantified by OARSI scoring (Figure 6, J–N). Subchondral bone and synovitis OARSI scores between surgical knees of Cre$^-$ and β-catenin active mice (*Ctnnb1$^{ex3fl/+}$ Col2-CreERT2*) were not significantly different. There was also no significant difference in OARSI scores for cartilage, subchondral bone, or synovitis in contralateral limbs from Cre$^-$ and *Ctnnb1$^{ex3fl/+}$ Col2-CreERT2* mice (Figure 6, J, L, N, and Supplemental Figure 6, B and D). Qualitatively, we also found that removal of the medial meniscus induced cellular changes consistent with OA, similar to our nonsurgical joint degeneration model and that, consistent with our nonsurgical model, activation of β-catenin reduced the observed surgically induced cellular phenotypes (Supplemental Table 1).

Consistent with the domain of X-gal staining of *R26RLacZ$^{fl/+}$ Col2-CreERT2* mice 6 weeks after tamoxifen injection, we found focal cartilage degeneration in the superficial and midzones of the cartilage in *SmoM2$^{fl/+}$ Col2-CreERT2* mice (Figure 6B and Supplemental Figure 6A). In addition, we found that mice that carried the *Ctnnb1^{ex3}* allele had increased nuclear staining of β-catenin in SFZ cells by immunohistochemistry (Supplemental Figure 5, B–D), suggesting recombination-induced expression of the *Ctnnb1^{ex3}* transgene within the same region. Interestingly, mice with conditionally activated hedgehog signaling (*SmoM2$^{fl/+}$ Col2-CreERT2)* or Cre$^-$ mice with surgically induced OA had reduced FGF18

Table 1. Pearson's correlation coefficients of RNA levels from human chondrocytes derived from femoral condyles obtained at knee replacement surgery

	ADAMTS4	AXIN2	TCF4
dnTCF4	0.408; $P = 0.028^A$	−0.454; $P = 0.013^A$	0.557; $P = 0.002$
TCF4	0.259; $P = 1.67$	−0.391; $P = 0.033^A$	NA

Correlation coefficients greater than 0.5 were considered very strong correlations, and those from 0.3 to 0.5 or from −0.3 to −0.5 were considered strong correlations. Data represent correlation coefficients. [A]Significant correlation ($P < 0.05$). dnTCF4 vs. other all other genes, $n = 29$. TCF4 vs. all other genes, $n = 30$.

compared with Cre⁻ mice or contralateral limbs, respectively (Figure 6, F, G, O, and P). Activation of β-catenin in mice with active hedgehog signaling (*SmoM2$^{fl/+}$ Ctnnb1$^{ex3fl/+}$ Col2-CreERT2)* rescued FGF18 expression across the articular surface (Figure 6I), consistent with our observations developmentally. However, in surgically induced OA mouse models, we did not observe FGF18 expression in mice with active β-catenin (*Ctnnb1$^{ex3fl/+}$ Col2-CreERT2;* Figure 6R); this was possibly a result of increased cartilage degeneration in surgical *Ctnnb1$^{ex3fl/+}$ Col2-CreERT2* mice compared with nonsurgical *SmoM2$^{fl/+}$ Ctnnb1$^{ex3fl/+}$ Col2-CreERT2* mice. We did observe sustained expression of ADAMTS5 in the articular cartilage of *Ctnnb1$^{ex3fl/+}$ Col2-CreERT2* surgically induced OA mice, similar to contralateral knees of Cre⁻ and *Ctnnb1$^{ex3fl/+}$ Col2-CreERT2* mice and in contrast with Cre⁻ surgically induced OA knees (Supplemental Figure 5, E–H). Overall, these results suggest that activation of β-catenin in surgical models of OA delays cartilage degeneration, possibly by maintaining FGF18 expression.

To determine whether our developmental and in vitro findings also related to human OA, we examined the expression of selected genes in osteoarthritic cartilage sampled from human femoral condyles at the time of knee-replacement surgery (Table 1). We found that there was a strong, positive, and significant correlation of *dnTCF4* with *ADAMTS4*, the major aggrecanase associated with human OA cartilage and not expressed in normal cartilage (29), consistent with our results when we overexpressed dnTCF4 in human chondrocytes (Figure 4K). Full-length *TCF4* did not significantly correlate with *ADAMTS4* expression. Furthermore, we found a substantial negative correlation between *AXIN2* and both full-length *TCF4* and *dnTCF4*, suggesting that increased expression of both of these factors could negatively regulate downstream β-catenin target gene expression. Finally, we also found that both *TCF4* and *dnTCF4* correlated significantly and very strongly with each other, consistent with protein changes observed when mouse costal chondrocytes were treated with PM (Figure 4A). Overall, these data suggest that the expression of dnTCF isoforms is linked to *ADAMTS4* expression and may play a vital role in initiating and regulating cartilage degeneration. Together, these studies indicate that it is necessary to maintain WNT/β-catenin activity at a high level in order to sustain joint integrity and, consistent with our findings in development, β-catenin target genes are likely modulated selectively by the increased expression of hedgehog-induced negative regulators, such as dnTCR7L2/dnTCF4, in OA.

Discussion

Here, we show that hedgehog signaling regulation plays a vital role in joint development and morphogenesis. Activation of hedgehog signaling in interzone cell progeny results in changes to joint morphogenesis and skeletal development. We found that hedgehog signaling is a negative regulator of chondrocyte differentiation at the articular surface and of selected β-catenin target gene expression through induction of negative regulators of β-catenin–mediated, TCF-dependent transcription, including TCF7L2/TCF4 isoforms. We identified β-catenin–induced FGF18 as an important factor responsible for maintaining joint morphogenesis when hedgehog is active in interzone progeny. Our findings in development also apply to joint degeneration, revealing a vital link between joint development and the maintenance of adult articular cartilage. We propose a model for the interaction between hedgehog and β-catenin signaling in which the balance of these pathways plays a vital role in regulating both joint development and disease (Figure 7).

Previous studies show morphological joint changes, including joint fusions, in response to *Ihh* expression or hedgehog activation by Cre-mediated recombination induced in *Col2a1*-expressing mesenchymal cells of transgenic mice (12, 30). The expression of *Col2a1* and *Col2a1-Cre* is upregulated in interzone progenitors prior to *Gdf5* expression or *Gdf5-Cre*-recombinase activity (31–33), targeting joint progenitor cells prior to interzone differentiation. We utilized *Gdf5-Cre* mice to spatially and temporally target interzone cells and their progeny, allowing us to modulate hedgehog signaling after interzone cell differentiation. This allowed for the integration of the effects of hedgehog signaling on the maintenance and differentiation of interzone progeny rather than on *Col2a1*-expressing cells before interzone cell differentiation. In contrast with joint fusions induced by early hedgehog activation reported in these previous studies, we observed undifferentiated cells within the knee joints. Thus, joint fusions may result from hedgehog-induced signaling factors expressed from the surrounding tissues and not directly in the interzone cells or their progeny.

Ihh-knockout mice fail to form joints in the distal digits of the hind limbs, but express *Gdf5* and other joint markers in areas surrounding sites predicted to form joints (13). In our study, removal of hedgehog signaling in interzone progeny (*Smo$^{fl/fl}$ Gdf5-Cre*) did not result in morphological changes to joint formation, suggesting that once *Gdf5*-expressing interzone cells form, hedgehog signaling in interzone progeny is dispensable for joint and skeletal morphogenesis up until birth.

IHH induces PTHLH expression in periarticular cells, which maintain proliferation, and delays terminal differentiation of growth plate chondrocytes (30, 34). We found that hedgehog activation in interzone progeny induced *Pthlh* expression, which explains the increased size of the growth plate and the reduced number of hypertrophic cells in the type X collagen domain. FGF18, expressed by cells in the developing joint and by perichondrial cells, also plays an important role in regulating growth plate maturation. FGF18 prevents maturation of resting and proliferating chondrocytes and promotes terminal maturation of hypertrophic chondrocytes (20, 35). *Fgf18* is also expressed in the perichondrium and contributes to the regulation of growth plate maturation (36). Although we did not observe changes in

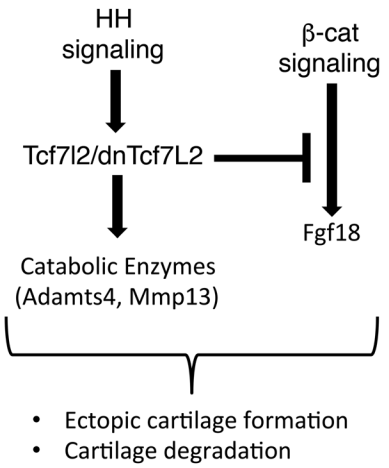

Figure 7. Summary of interaction between hedgehog and β-catenin signaling in interzone progeny and articular chondrocytes. In interzone progeny during development, hedgehog (HH) signaling induces the expression of TCF7L2 (and human TCF4) isoforms, including dominant negative isoforms. Increased expression of TCF7L2 protein isoforms limits signaling by β-catenin (β-cat), resulting in an inhibition of expression of FGF18, leading to ectopic cartilage formation. In adult chondrocytes, HH signaling activity induces cartilage degeneration. Expression of dnTCF7L2 and other TCF7L2 isoforms induces the expression of catabolic enzymes, including ADAMTS4 and MMP13, which are involved in cartilage degeneration as part of OA. Increasing β-catenin activity rescues hedgehog-induced ectopic cartilage formation and cartilage degradation, likely by restoring the balance between HH and β-catenin signaling.

Fgf18 expression in the perichondrium (Supplemental Figure 4, M and N), the growth plate phenotypes and loss of *Fgf18* expression observed in mice with active hedgehog signaling from our current study are consistent with the described role of FGF18 in regulating growth plate maturation. This suggests that FGF18 expressed from interzone progeny regulates interzone-to-chondrocyte differentiation and may signal, in concert with the perichondrium, to regulate growth plate maturation.

Although activation of β-catenin rescued expression of *Fgf18* in interzone progeny of mice with constitutive hedgehog signaling, we saw only partial rescue of growth plate length (Supplemental Figure 2I), likely the result of the sustained expression of PTHLH induced in vivo (Supplemental Figure 4H). This raises the possibility that the effect of hedgehog activation on growth plate chondrocyte maturation, as seen in other studies (1, 12), may be dependent on both increased PTHLH and reduced FGF18 expression. In addition, in this study, FGF18 but not FGF4 inhibited ectopic cartilage formation in mice with active hedgehog signaling in interzone progeny. Since FGF18 primarily signals through FGFR3, whereas FGF4 has low signaling through this receptor (37, 38), signaling through FGFR3 likely inhibits ectopic cartilage formation. This is consistent with recent studies that show that inhibition of FGFR3 signaling in chondrocytes can promote hedgehog signaling and induce chondroma-like lesions (39). However, we found that FGF18 alone could not inhibit all hedgehog-mediated phenotypes, including the persistence of undifferentiated cells in the joint space (Figure 5O), possibly as a result of sustained hedgehog-induced gene expression.

Previous studies show that WNT/β-catenin signaling induces differentiation of interzone cells and maintains progeny in vivo (6, 10). Since we showed selective reduction in β-catenin target gene expression with active hedgehog signaling in vitro and in vivo, we propose that hedgehog signaling in interzone progeny may prime these cells to become more mesenchymal-like and prone to signals from surrounding tissues for differentiation into progeny including chondrocytes. Interestingly, we only observed ectopic cartilage on the tibia and a loss of meniscus formation within the knee as a result of hedgehog signaling in interzone progeny. The selective location of the ectopic cartilage may be a result of morphogen or mechanical signals coming from surrounding tissues, possibly the patellar ligament, leading to local differentiation, as described in tendon-influenced bone eminence formation (40, 41). The loss of meniscus formation may result from proliferation of the interzone progeny in the joint space, as identified by Ki67 staining in this study, rather than differentiation, or through dysregulation of multiple genes directing the differentiation of the meniscus (42). However, the specific signals disrupting meniscus formation and selective ectopic cartilage formation observed in this study require further investigation.

Our work in mice identified selective changes to the mRNA expression of the β-catenin target gene *Fgf18* but not *Axin2* in vivo and in vitro in response to hedgehog activation without alteration of β-catenin localization in vivo. Previous studies show that hedgehog and WNT/β-catenin signaling interact and negatively regulate β-catenin target gene expression through expression of secreted frizzled-related proteins (43) or through expression of intracellular TCF/LEF transcription factors including dnTCF7L2/dnTCF4 (16). We determined that both dominant negative and full-length isoforms of TCF7L2 are expressed in vivo and in vitro and are responsible, in part, for reductions in *Fgf18* expression, as determined in our costal chondrocyte cultures. Full-length TCF7L is expressed by developing chondrogenic condensations within the developing limb and binds to β-catenin–regulated target genes, including *Axin2* and *Fgf18*, within promoter or intronic regions (18, 19, 26, 44). All TCF transcription factors bind to transcriptional corepressors, which are then displaced in response to accumulation of nuclear β-catenin (45, 46). In response to WNT ligands, TCF transcription factors have varying abilities to control target gene expression based on cell type, epigenetic state, and TCF/LEF binding ability (47, 48). For example, *Axin2* shows less selectivity for specific TCF isoforms needed for WNT-induced transcription, whereas *T/Bra* is more stringent in its TCF-binding complement for WNT-induced transcription (48). Interestingly, full-length TCF4, but not LEF1 or TCF3, induces MMP1, MMP3, and MMP13 expression in human chondrocytes in vitro and is upregulated in human OA cartilage compared with healthy cartilage in vivo (49). This can be explained by increased TCF4-corepressor complexes forming due to the limited pool of β-catenin able to bind to TCF4, which overall promotes *Mmp* gene expression, similar to our results from overexpression of dnTCF4 in human chondrocytes.

The number of TCF-binding elements in a gene could also play a role in transcriptional regulation. Mouse *Axin2* has 8 TCF-binding sites within exon 1 and intron 1 that regulate gene expression in response to WNT activation (44). In contrast, mouse *Fgf18* has

a single site within the promoter region necessary for activation (18, 19). Overall, this suggests that mouse *Axin2* would be less sensitive to regulation by TCF transcription factor isoforms, such as corepressor-bound TCF7L2 and dnTCF7L2, than *Fgf18*, consistent with observations in this study. Interestingly, only 5 of the 8 TCF-binding sites in the mouse *Axin2* gene are conserved in human *AXIN2* (44), suggesting that human *AXIN2* may be more sensitive to changes in TCF4 isoform expression, which we observed in our dnTCF4 overexpression study and analysis of human chondrocytes as compared with our in vitro studies in mouse chondrocytes (Figure 4, B and G; Supplemental Figure 4J; and Table 1).

There are conflicting data in the literature concerning the effect of modulation of β-catenin activity on articular stability. Inhibition of β-catenin in chondrocytes results in cartilage degeneration and hallmarks of OA, including chondrocyte clusters and ectopic bone (50). Stabilization of β-catenin in chondrocytes also induces an OA-like phenotype (51). Osteoarthritic cartilage has increased β-catenin protein within the chondrocytes (51); however, how this changes β-catenin–mediated gene expression in OA has not been defined. Our developmental data suggest that there may be selective changes to gene expression in interzone progeny, which may translate to gene-expression changes and phenotypes seen in OA. In our study, hedgehog activation in interzone progeny resulted in ectopic cartilage formation, a phenotype similar to the ectopic bone seen in adult mice with inhibition of β-catenin (50). In contrast to previously published work (51), we did not observe structural damage to the knee-joint cartilage with β-catenin stabilization in chondrocytes of mature mice. This could be a result of stabilization of β-catenin in younger mice compared with that found in previous studies, due to timing of analysis of the joint after β-catenin stabilization or the lower recombination efficiency seen in our study. However, we still observed marked rescue of our OA phenotypes with activation of *Ctnnb1*^{ex3}, suggesting that a secreted factor may be responsible for the reduction in cartilage damage. We also found that constitutive activation of β-catenin sustained FGF18 expression in hedgehog-induced models of cartilage degeneration. Interestingly, intraarticular injection of recombinant FGF18 can repair surgically induced cartilage degeneration in rats (52). Although we did not observe FGF18 expression in *Ctnnb1*^{ex3} *Col2-CreERT2* mice with surgically induced OA, this may be a result of the severity of OA induced by the medial meniscectomy surgery. A less severe surgical model of OA that can be observed more longitudinally, such as the DMM model of OA, may be more suitable for studying the interaction between β-catenin and FGF18 during OA pathogenesis. Overall, however, our data and that from Moore et al. (52) would suggest that expression and signaling from β-catenin–induced FGF18 in the joint is necessary not only for repair, but also for joint maintenance.

We found a selective correlation of *ADAMTS4* with *dnTCF4*, but not full-length *TCF4*, in human chondrocytes. However, *AXIN2* negatively correlated with the expression of both *dnTCF4* and full-length isoforms. Thus, similarly to our results in development, hedgehog signaling in OA may selectively regulate target genes through expression of *dnTcf7l2/dnTCF4*, augmenting the transcriptional response to WNT-induced β-catenin activity, preventing the maintenance of progenitor cells in the joint, and inducing cartilage degradation. Therefore, investigations identifying the overall transcriptional changes induced by hedgehog integration with β-catenin signaling will likely help to define molecular pathways regulating not only developmental processes, but also pathological disease states. Finally, consistent with conclusions drawn from other groups (21, 50), our data also support the notion that treatment modalities that upregulate β-catenin activity may help to attenuate articular cartilage destruction in OA.

Methods

Mice. *Gdf5-Cre* mice (a gift from D. Kingsley, Stanford University School of Medicine, Stanford, California, USA; ref. 32) were used to drive recombinase activity in interzone cells. To study the effect of inhibition and activation of hedgehog signaling in interzone progeny, we generated *Smo*$^{fl/fl}$ *Gdf5-Cre* (53), *Ptch1*$^{fl/fl}$ *Gdf5-Cre* (54), and *SmoM2*$^{fl/+}$ *Gdf5-Cre* mice (55) (which express a constitutively active Smo from the *R26R* locus upon Cre-mediated recombination; *Smo*$^{fl/fl}$, *Ptch1*$^{fl/fl}$, and *SmoM2*$^{fl/+}$ mice were gifts from C.C. Hui, Hospital for Sick Children, Toronto). We utilized *Ctnnb1*$^{ex3fl/fl}$ mice (a gift from M. Taketo, Kyoto University, Kyoto, Japan; ref. 56), which express a constitutively active form of β-catenin upon Cre-mediated recombination. We generated *Ctnnb1*$^{ex3fl/+}$ *Gdf5-Cre* and *SmoM2*$^{fl/+}$ *Ctnnb1*$^{ex3fl/+}$ *Gdf5-Cre* mice to investigate the interaction between active hedgehog and canonical WNT/β-catenin signaling in interzone progeny. For lineage tracing, we generated *R26RLacZ*$^{fl/fl}$ (Gt[ROSA]26tm1Sor, The Jackson Laboratory; ref. 57) *Gdf5-Cre* and *SmoM2*$^{fl/+}$ *R26RLacZ*$^{fl/fl}$ *Gdf5-Cre* mice. Embryos were considered E0.5 on date of vaginal plug. Embryos or neonatal mice were collected between E12.5 and P0.

Col2-CreERT2 mice (a gift from D. Chen, Rush University, Chicago, Illinois, USA; ref. 51) were used to drive tamoxifen-induced recombinase activity in chondrocytes of postnatal mice. *SmoM2*$^{fl/+}$ *Col2-CreERT2*, *Ctnnb1*$^{ex3fl/+}$ *Col2-CreERT2*, *SmoM2*$^{fl/+}$ *Ctnnb1*$^{ex3fl/+}$, *Col2-CreERT2*, *R26RLacZ*$^{fl/+}$ *Col2-CreERT2*, and Cre$^-$ mice were generated. For mice that did not undergo surgery, tamoxifen (1 mg/10 g; Sigma-Aldrich) was injected in 8-week-old mice for 5 consecutive days, as previously described (51). Mice were sacrificed 6 weeks after injection. Medial meniscectomy was performed on the left hind limb of some *Ctnnb1*$^{ex3fl/+}$ *Col2-CreERT2* and Cre$^-$ littermates at 8 weeks of age. Six days after surgery, mice were injected with tamoxifen and sacrificed 6 weeks after injection. Severity of cartilage degeneration on the medial surface of the tibia, synovitis, and tibial subchondral bone thickening was assayed by OARSI scoring recommended for analysis of mouse OA (28). Between 3 and 8 sections from 2 to 4 slides separated by a minimum of 60 μm were evaluated by 3 independent, blinded reviewers, and the mean score for each joint compartment was determined.

Whole-mount and histological staining. For whole-mount skeleton preparations, P0 mice were skinned, eviscerated, and fixed in 95% ethanol. Mice were stained with Alcian blue (0.015% in acetic acid/95% ethanol at a ratio of 1:4) for cartilage, cleared with 1%–2% KOH, then stained again with Alizarin red for bone (0.005% in 1% KOH).

E14.5 or E17.5 embryonic hind limbs were fixed in formalin and embedded in paraffin. Histological sections were stained by SafO/Fast Green/Weigert's iron hematoxylin to identify proteoglycan-rich cartilage, or von Kossa/Nuclear Fast Red to identify calcified tissue. Adult mouse hind limbs were fixed in 10% formalin and decalcified using 3 changes of Immunocal (Decal Chemical Corp.) over 5 days. Hind limbs

were postfixed in 10% formalin, embedded in paraffin, sectioned, and stained with SafO/Fast Green/Weigert's iron hematoxylin.

E14.5 and E17.5 *R26RLacZ*$^{fl/fl}$ *Gdf5-Cre* or *SmoM2*$^{fl/fl}$ *R26RLacZ*$^{fl/fl}$ *Gdf5-Cre* embryos and tamoxifen-injected *R26LacZ*$^{fl/+}$ *Col2-CreERT2* mice were fixed for 2 hours in 4% formaldehyde, 0.02% NP40, in PBS at pH 7.3 at 4°C, washed 3 times in 2 mM $MgCl_2$, 0.02% NP-40, in PBS at pH 7.3, and stained in wash buffer containing 1 mg/ml X-gal, 5 mM $K_3Fe(CN)_6$,and 5 mM $K_4FE(CN)_6$ $3H_2O$. Limbs were washed with PBS and postfixed in 10% formalin. Adult limbs were decalcified using 3 changes of Immunocal for 5 days. Limbs were then paraffin embedded, and histological sections (5 μm) were counterstained with Nuclear Fast Red.

The length of long-bone cartilage and ossified regions, the total, proliferative, prehypertrophic, and hypertrophic length of the growth plate, the average length of the dorsal and ventral sides of the bone collar surrounding the growth plate, the area of X-gal–stained chondrocytes, and the number of cells expressing in situ hybridization markers or X-gal staining were measured by histomorphometry.

In situ hybridization and immunohistochemistry. Antisense RNA probes for *Sox9* and *Col2a1* (a gift from C.C. Hui; ref. 58), markers of chondrocytes, *Col1a1* (a gift from S. Takedo, Tokyo Medical and Dental University, Tokyo, Japan; ref. 59), a marker of osteoblasts and undifferentiated mesenchymal cells, *Fgf18* (a gift from D. Ornitz, Washington University School of Medicine, St. Louis, Missouri, USA; ref. 20) and *Axin2* (a gift from C.C. Hui; ref. 44), TCF/LEF–β-catenin complex targets, *Ptch1* (60) and *Pthlh* (gifts from C.C. Hui; ref. 61), and hedgehog-induced target genes were prepared by in vitro transcription using digoxigenin-labeled UTP (Roche) per the manufacturer's instructions. dnTCF7L2 probes were generated by PCR using cDNA templates generated (Superscript II; Invitrogen Life Technologies) from RNA isolated (RNeasy Mini Kit; QIAGEN) from the head of E13.5 CD1 embryos and previously described primers (1b isoform; ref. 16). Formalin-fixed, paraffin-embedded histological sections (5 μm) from hind limbs of E14.5–E17.5 mice were treated with proteinase K for 20 minutes, postfixed in 4% PFA, and hybridized with probes for approximately 16 hours at 55°C, as previously described. HRP-tagged anti-digoxigenin Fc antibody fragments (11093274910, Roche) were bound to sections overnight at 4°C and stained with BM Purple (Roche). Sections were counterstained with Nuclear Fast Red.

For immunohistochemistry, dehydrated, paraffin-embedded sections from hind limbs of E14.5, E17.5, or adult mice were rehydrated. For E14.5 and E17.5 sections, antigen retrieval was performed by boiling in 10 mM citrate buffer (pH 6.0). For adult mice, antigen retrieval was performed by incubation of sections in 0.1% pepsin (Sigma-Aldrich) in 0.5 M acetic acid for 30 minutes or overnight in 10 mM citrate buffer (pH 6.0) at 60°C. E17.5 sections were incubated overnight at 4°C with rat anti-mouse Ki67 monoclonal antibody (clone TEC-3; M7249, Dako), a marker of proliferation. Adult sections were similarly incubated with anti-FGF18 (HPA018795, Sigma-Aldrich) or anti-ADAMTS5 (AB41037, Abcam) antibodies. For β-catenin immunohistochemistry, E14.5 or adult sections were prepared using the M.O.M. Kit (Vector Laboratories) and incubated at 4°C overnight with mouse anti–β-catenin monoclonal antibody (clone 14; 610154, BD Biosciences). E17.5 hind limb sections were enzymatically digested and stained for type X collagen (clone X53; 1-CO097-05, Quartett), as previously described (62). For all immunohistochemistry, sections were incubated with appropriate HRP-conjugated secondary antibodies and ABC solution prior to color reaction using DAB Substrate Kit (all from Vector Laboratories). Sections were counterstained with Mayer's hematoxylin.

In vitro cell culture, immunoblotting, and qPCR. SFZ cells were isolated on tissue culture plastic coated with cellular fibronectin from human foreskin fibroblasts (Sigma-Aldrich) from knees of 3 independent litters of 4- to 5-day-old CD1 pups (Toronto Centre for Phenogenomics), as previously described (63). Cells were cultured in serum-free DMEM (Wisent Bioproducts) overnight prior to culture with PM (5 μM, 10009634, Cayman Chemical) and/or WNT3a (canonical WNT/β-catenin agonist; 100 ng/ml; R&D Systems). RNA was isolated using TRIzol (Invitrogen) followed by RNeasy Mini Kit columns. RNA was reverse transcribed by Superscript II. β-Catenin and hedgehog target gene expression from the cultures (*Axin2* or *Fgf18* and *Ptch1*, respectively) were determined by qPCR relative to the expression of eukaryotic 18S rRNA using TaqMan Universal PCR Master Mix and commercially available TaqMan primers/probes (*Axin2*, Mm00443610_m1; *Fgf18*, Mm00433286_m1; *Ptch1*, Mm00436026_m1; 18S rRNA, 4352930; Applied Biosystems).

Murine costal chondrocytes were isolated from P5 C57BL/6J mice (The Jackson Laboratory), as previously described (21). Cells were seeded onto tissue culture plastic at a density of 5×10^4 cells/cm^2 in DMEM containing 10% FBS and 1% penicillin/streptomycin. Cells were cultured for 60 hours prior to treatment with DMSO or 10 μM PM. Cell were then transfected with 10 nM Silencer Select Pre-Designed siRNA Tcf7l2-T1 (s74839-exons 4–6) or Silencer Select Negative Control no. 1 siRNA (4390843, Invitrogen) using Lipofectamine RNAiMAX (Invitrogen). Total RNA was isolated 48 hours after treatment and transfection using TRIzol. cDNA was synthesized using iScript Reverse Transcription Supermix for real-time reverse transcription qPCR (RT-qPCR) (Bio-Rad Laboratories Inc.). Gene-expression assays were conducted to determine the expression of β-catenin and hedgehog target gene (*Axin2* or *Fgf18*, and *Gli1*, respectively) relative to β-actin, using SsoAdvanced Universal Probes Supermix (Bio-Rad Laboratories). Primer sequences used for qPCR of primary mouse chondrocytes were as follows: *Actb* (F: GGCTGTATTCCCCTCCATCG, R: CCAGTTGGTAACAATGCCATGT); *Gli1* (F: CCACAGGCACACAGGATCACC, R: ACAGACTCAGGC TCAGGCTTCTC);*Fgf18* (F; TGAACACGCACTCCTTGCTAGT, R: GAATTCTACCTGTGTATGAACCGAAA); and *Axin2* (F: TGTTTCTTACTCCCCATGCG, R: ATGTCTTTGCACCAGCCA).

Tissue samples of human articular cartilage were obtained from 5 patients with OA at the time of total knee arthroplasty. Cartilage was dissected away from the underlying bone under sterile conditions, washed twice with PBS, and incubated in 1 mg/ml pronase solution (Roche) for 30 minutes at 37°C in DMEM/F12 supplemented with 10% FBS, 1% penicillin/streptomycin, 0.1% ITS (R&D system), and 50 μg/ml L-ascorbic acid (Sigma-Aldrich). Samples were plated in 1 mg/ml collagenase P solution (Roche) in complete media at 37°C overnight. The cell suspension was filtered through a 70-μm filter, centrifuged for 3 minutes at 800 *g*, and resuspended in culture medium. For culture, the chondrocytes were seeded in high-density monolayer (1.0×10^5 cells/cm^2).

Human chondrocytes were infected with an adenovirus expression vector for human dominant negative TCF4 (Vector Biolabs) or an adenovirus-GFP (control, Vector Biolabs) for 24 hours at 50 MOI and replaced in fresh medium. Cells infected with vectors were collected

after 72 hours. Total RNA was isolated using the RNeasy Mini Kit (QIAGEN), and cDNA was generated using PrimeScript RT Reagent Kit with gDNA Eraser (Takara Bio). qPCR was performed using SYBR Premix EX Taq (Tli RNaseH Plus; Takara Bio) to determine the expression of selective β-catenin target genes (*AXIN2* and *FGF18*), genes associated with cartilage catabolism (*MMP13*, *MMP3*, and *ADAMTS4*), and *TCF4* relative to the expression of *HPRT*. The following primer sets were used for qPCR of adenoviral-infected primary human chondrocytes: *TCF4* (F: ATCCTTGCCTTTCACTTCCTC, R: AGCTGCCTTCACCTTGTATG); *AXIN2* (F: ATGTCTTTGCACCAGCCA, R: TGTTTCTTACTCCCCATGCG); *FGF18*, (R: AAGTATGCCCAGCTCCTAGT, R: GATGAACACACACTCCTTGCT); *MMP3* (F: GACAAAGGATACAACAGGGACCAAT, R: TGAGTGAGTGATAGAGTGGGTACAT); *MMP13* (F: GTCTCTCTATGGTCCAGGAGATGAA, R: AGGCGCCAGAAGAATCTGT); *ADAMTS4* (F: TCACTGACTTCCTGGACAATGG, R: ACTGGCGGTCAGCATCATAGT); and *HPRT* (F: GAAAAGGACCCCACGAAGTGT, R: AGTCAAGGGCATATCCTACAA).

Protein from siRNA-transfected or adenoviral vector–infected cells was extracted using RIPA buffer containing protease inhibitors. Protein (30 μg) was separated by electrophoresis in 10% SDS-PAGE gels and transferred onto nitrocellulose membranes. Immunoblots were probed with rabbit anti-TCF4 (clone C48H11; 2569, Cell Signaling) or mouse anti–β-actin loading control monoclonal antibodies (clone BA3R; MA5-15739, Pierce), followed by anti-rabbit or anti-mouse HRP-conjugated secondary antibodies (Vector Laboratories), and exposed using Supersignal West Pico chemiluminescent substrate (Pierce).

RNA was extracted from human osteoarthritic chondrocytes isolated from the femoral condyles at time of total joint replacement surgery. Gene-expression levels of *AXIN2* and *ADAMTS4* were determined by qPCR relative to *ACTB* using TaqMan Universal PCR Master Mix and commercially available TaqMan primer/probes (*AXIN2*, Hs00394718_m1; *ADAMTS4*, Hs00192708_m1; *ACTB*, Hs01060665_g1; Applied Biosystems). Gene-expression levels of total *TCF7L2* and *dnTCF7L2* (1b isoform) were determined by qPCR relative to *HPRT* expression using SYBR Green PCR Master Mix (Applied Biosystems) and previously defined primers (64). Undetermined Ct values were set to 50 (the maximum cycle number for the qPCR run) prior to analysis.

Ex vivo hind limb culture. Limbs from E14.5 *SmoM2*$^{fl/+}$ *Gdf5-Cre* or Cre^{-} mice were cultured on nucleopore filters (Fisher Scientific) in serum-free DMEM supplemented with vehicle, 200 ng/ml hrFGF18, or 200 ng/ml hrFGF4 (Peprotech Inc.). Supplemented media was changed after 24 hours, and limbs were fixed in 10% formalin at 48 hours. Hind limbs were embedded in paraffin, sectioned (5 μm), and stained with SafO/Fast Green/Weigert's iron hematoxylin.

Statistics. Data are reported as mean ± 95% CI or SEM. Data normalized to control or presented as percentage were log transformed prior to statistical analysis. Data were analyzed by 2-tailed Student's *t* tests, paired *t* tests, 1-way ANOVA followed by Tukey's post-hoc tests, repeated-measures ANOVA followed by Tukey's post-hoc tests, or Pearson's correlation using Prism (Graphpad Software Inc). Statistical significance was determined as $P < 0.05$.

Study approval. Animal use was approved by the Animal Care Committee at the Toronto Centre for Phenogenomics. Informed consent was obtained for use of human tissue samples with approval from the Mount Sinai Hospital Research Ethics Board (Toronto, Ontario, Canada; REB no. 01-0142-A) and from the Duke University Research Ethics Board (Durham, NC, USA; IRB no. Pro00016105).

Author contributions

JSR conceived and designed research studies, conducted experiments, acquired and analyzed data, and wrote the manuscript. CY conducted experiments and acquired and analyzed data. HW conducted experiments, acquired and analyzed data, and edited the manuscript. AMC designed research studies, conducted experiments, and acquired and analyzed data. KR, HM, HT, and VP conducted experiments and acquired and analyzed data. MAJ analyzed data. GMK and BAA conceived and designed research studies. BA also edited the manuscript.

Acknowledgments

This work was supported by a grant from the Canadian Institutes of Health Research (MOP-106587). Research reported in this publication was also supported in part by the National Institute of Arthritis and Musculoskeletal and Skin Diseases of the NIH under award number R0 AR066765 01. The content is solely the responsibility of the authors and does not necessarily represent the official views of the NIH. J.S. Rockel was supported by fellowships from the Hospital for Sick Children and the Toronto Musculoskeletal Centre.

Address correspondence to: Benjamin A. Alman, Department of Orthopaedic Surgery, Duke University, DUMC 2888, 200 Trent Drive, Orange Zone 5th floor, Durham, North Carolina 27710, USA. Phone: 919.613.6935; E-mail: ben.alman@duke.edu.

Jason S. Rockel's present address is: Division of Genetics and Development, Krembil Research Institute, University Health Network, Toronto, Ontario, Canada.

April M. Craft's present address is: Orthopaedic Research Laboratories, Children's Hospital Boston, Boston, Massachusetts, USA.

Katherine Reilly's present address is: Department of Cellular and Molecular Medicine, University of Ottawa, Ottawa, Ontario, Canada.

1. Kobayashi T, et al. Indian hedgehog stimulates periarticular chondrocyte differentiation to regulate growth plate length independently of PTHrP. *J Clin Invest*. 2005;115(7):1734–1742.
2. Rhee DK, et al. The secreted glycoprotein lubricin protects cartilage surfaces and inhibits synovial cell overgrowth. *J Clin Invest*. 2005;115(3):622–631.
3. Gelse K, Soder S, Eger W, Diemtar T, Aigner T. Osteophyte development — molecular characterization of differentiation stages. *Osteoarthritis Cartilage*. 2003;11(2):141–148.
4. Lin AC, et al. Modulating hedgehog signaling can attenuate the severity of osteoarthritis. *Nat Med*. 2009;15(12):1421–1425.
5. Zhen G, et al. Inhibition of TGF-β signaling in mesenchymal stem cells of subchondral bone attenuates osteoarthritis. *Nat Med*. 2013;19(6):704–712.
6. Koyama E, et al. A distinct cohort of progenitor cells participates in synovial joint and articular cartilage formation during mouse limb skeletogenesis. *Dev Biol*. 2008;316(1):62–73.
7. Dy P, et al. Synovial joint morphogenesis requires

the chondrogenic action of Sox5 and Sox6 in growth plate and articular cartilage. *Dev Biol*. 2010;341(2):346–359.
8. Hyde G, Boot-Handford RP, Wallis GA. Col2a1 lineage tracing reveals that the meniscus of the knee joint has a complex cellular origin. *J Anat*. 2008;213(5):531–538.
9. Später D, Hill TP, Gruber M, Hartmann C. Role of canonical Wnt-signalling in joint formation. *Eur Cell Mater*. 2006;12:71–80.
10. Guo X. Wnt/β-catenin signaling is sufficient and necessary for synovial joint formation. *Genes Dev*. 2004;18(19):2404–2417.
11. Spagnoli A, et al. TGF-β signaling is essential for joint morphogenesis. *J Cell Biol*. 2007;177(6):1105–1117.
12. Mak KK, Chen M-H, Day TF, Chuang P-T, Yang Y. Wnt/β-catenin signaling interacts differentially with Ihh signaling in controlling endochondral bone and synovial joint formation. *Development*. 2006;133(18):3695–3707.
13. Koyama E, et al. Synovial joint formation during mouse limb skeletogenesis: roles of Indian hedgehog signaling. *Ann N Y Acad Sci*. 2007;1116:100–112.
14. Später D, Hill TP, O'Sullivan RJ, Gruber M, Conner DA, Hartmann C. Wnt9a signaling is required for joint integrity and regulation of Ihh during chondrogenesis. *Development*. 2006;133(15):3039–3049.
15. Yu W, McDonnell K, Taketo MM, Bai CB. Wnt signaling determines ventral spinal cord cell fates in a time-dependent manner. *Development*. 2008;135(22):3687–3696.
16. Vacik T, Stubbs JL, Lemke G. A novel mechanism for the transcriptional regulation of Wnt signaling in development. *Genes Dev*. 2011;25(17):1783–1795.
17. Singh BN, Doyle MJ, Weaver CV, Koyano-Nakagawa N, Garry DJ. Hedgehog and Wnt coordinate signaling in myogenic progenitors and regulate limb regeneration. *Dev Biol*. 2012;371(1):23–34.
18. Shimokawa T, et al. Involvement of the FGF18 gene in colorectal carcinogenesis, as a novel downstream target of the beta-catenin/T-cell factor complex. *Cancer Res*. 2003;63(19):6116–6120.
19. Reinhold MI, Naski MC. Direct interactions of Runx2 and canonical Wnt signaling induce FGF18. *J Biol Chem*. 2007;282(6):3653–3663.
20. Liu Z, Xu J, Colvin JS, Ornitz DM. Coordination of chondrogenesis and osteogenesis by fibroblast growth factor 18. *Genes Dev*. 2002;16(7):859–869.
21. Yasuhara R, et al. Roles of β-catenin signaling in phenotypic expression and proliferation of articular cartilage superficial zone cells. *Lab Invest*. 2011;91(12):1739–1752.
22. Mitchell PG, et al. Cloning, expression, and type II collagenolytic activity of matrix metalloproteinase-13 from human osteoarthritic cartilage. *J Clin Invest*. 1996;97(3):761–768.
23. Wu JJ, Lark MW, Chun LE, Eyre DR. Sites of stromelysin cleavage in collagen types II, IX, X, and XI of cartilage. *J Biol Chem*. 1991;266(9):5625–5628.
24. van Meurs J, et al. Cleavage of aggrecan at the Asn341-Phe342 site coincides with the initiation of collagen damage in murine antigen-induced arthritis: a pivotal role for stromelysin 1 in matrix metalloproteinase activity. *Arthritis Rheum*. 1999;42(10):2074–2084.
25. Tortorella MD, et al. Sites of aggrecan cleavage by recombinant human aggrecanase-1 (ADAMTS-4). *J Biol Chem*. 2000;275(24):18566–18573.
26. Cho EA, Dressler GR. TCF-4 binds β-catenin and is expressed in distinct regions of the embryonic brain and limbs. *Mech Dev*. 1998;77(1):9–18.
27. McNulty MA, Loeser RF, Davey C, Callahan MF, Ferguson CM, Carlson CS. Histopathology of naturally occurring and surgically induced osteoarthritis in mice. *Osteoarthritis Cartilage*. 2012;20(8):949–956.
28. Glasson SS, Chambers MG, Van Den Berg WB, Little CB. The OARSI histopathology initiative - recommendations for histological assessments of osteoarthritis in the mouse. *Osteoarthritis Cartilage*. 2010;18(suppl 3):S17–S23.
29. Naito S, et al. Expression of ADAMTS4 (aggrecanase-1) in human osteoarthritic cartilage. *Pathol Int*. 2007;57(11):703–711.
30. Mak KK, Kronenberg HM, Chuang PT, Mackem S, Yang Y. Indian hedgehog signals independently of PTHrP to promote chondrocyte hypertrophy. *Development*. 2008;135(11):1947–1956.
31. Nakamura E, Nguyen M-T, Mackem S. Kinetics of tamoxifen-regulated Cre activity in mice using a cartilage-specific CreERT to assay temporal activity windows along the proximodistal limb skeleton. *Dev Dyn*. 2006;235(9):2603–2612.
32. Rountree RB, et al. BMP receptor signaling is required for postnatal maintenance of articular cartilage. *PLoS Biol*. 2004;2(11):e355.
33. Storm EE, Kingsley DM. Joint patterning defects caused by single and double mutations in members of the bone morphogenetic protein (BMP) family. *Development*. 1996;122(12):3969–3979.
34. Vortkamp A, Lee K, Lanske B, Segre GV, Kronenberg HM, Tabin CJ. Regulation of rate of cartilage differentiation by Indian hedgehog and PTH-related protein. *Science*. 1996;273(5275):613–622.
35. Jacob AL, Smith C, Partanen J, Ornitz DM. Fibroblast growth factor receptor 1 signaling in the osteo-chondrogenic cell lineage regulates sequential steps of osteoblast maturation. *Dev Biol*. 2006;296(2):315–328.
36. Hinoi E, et al. Runx2 inhibits chondrocyte proliferation and hypertrophy through its expression in the perichondrium. *Genes Dev*. 2006;20(21):2937–2942.
37. Zhang X, Ibrahimi OA, Olsen SK, Umemori H, Mohammadi M, Ornitz DM. Receptor specificity of the fibroblast growth factor family. The complete mammalian FGF family. *J Biol Chem*. 2006;281(23):15694–15700.
38. Ornitz DM, et al. Receptor specificity of the fibroblast growth factor family. *J Biol Chem*. 1996;271(25):15292–15297.
39. Zhou S, et al. FGFR3 deficiency causes multiple chondroma-like lesions by upregulating Hedgehog signaling. *PLoS Genet*. 2015;11(6):e1005214.
40. Blitz E, Sharir A, Akiyama H, Zelzer E. Tendon-bone attachment unit is formed modularly by a distinct pool of Scx- and Sox9-positive progenitors. *Development*. 2013;140(13):2680–2690.
41. Blitz E, et al. Bone ridge patterning during musculoskeletal assembly is mediated through SCX regulation of Bmp4 at the tendon-skeleton junction. *Dev Cell*. 2009;17(6):861–873.
42. Pazin DE, Gamer LW, Capelo LP, Cox KA, Rosen V. Gene signature of the embryonic meniscus. *J Orthop Res*. 2014;32(1):46–53.
43. Katoh Y, Katoh M. WNT antagonist, SFRP1, is Hedgehog signaling target. *Int J Mol Med*. 2006;17(1):171–175.
44. Jho EH, Zhang T, Domon C, Joo CK, Freund JN, Costantini F. Wnt/β-catenin/Tcf signaling induces the transcription of Axin2, a negative regulator of the signaling pathway. *Mol Cell Biol*. 2002;22(4):1172–1183.
45. Daniels DL, Weis WI. β-Catenin directly displaces Groucho/TLE repressors from Tcf/Lef in Wnt-mediated transcription activation. *Nat Struct Mol Biol*. 2005;12(4):364–371.
46. Brantjes H, Roose J, van De Wetering M, Clevers H. All Tcf HMG box transcription factors interact with Groucho-related co-repressors. *Nucleic Acids Res*. 2001;29(7):1410–1419.
47. Wohrle S, Wallmen B, Hecht A. Differential control of Wnt target genes involves epigenetic mechanisms and selective promoter occupancy by T-cell factors. *Mol Cell Biol*. 2007;27(23):8164–8177.
48. Wallmen B, Schrempp M, Hecht A. Intrinsic properties of Tcf1 and Tcf4 splice variants determine cell-type-specific Wnt/β-catenin target gene expression. *Nucleic Acids Res*. 2012;40(19):9455–9469.
49. Ma B, Zhong L, van Blitterswijk CA, Post JN, Karperien M. T cell factor 4 is a pro-catabolic and apoptotic factor in human articular chondrocytes by potentiating nuclear factor κB signaling. *J Biol Chem*. 2013;288(24):17552–17558.
50. Zhu M, et al. Inhibition of β-catenin signaling in articular chondrocytes results in articular cartilage destruction. *Arthritis Rheum*. 2008;58(7):2053–2064.
51. Zhu M, et al. Activation of β-catenin signaling in articular chondrocytes leads to osteoarthritis-like phenotype in adult β-catenin conditional activation mice. *J Bone Miner Res*. 2009;24(1):12–21.
52. Moore EE, et al. Fibroblast growth factor-18 stimulates chondrogenesis and cartilage repair in a rat model of injury-induced osteoarthritis. *Osteoarthritis Cartilage*. 2005;13(7):623–631.
53. Long F, Zhang XM, Karp S, Yang Y, McMahon AP. Genetic manipulation of hedgehog signaling in the endochondral skeleton reveals a direct role in the regulation of chondrocyte proliferation. *Development*. 2001;128(24):5099–5108.
54. Ellis T, et al. Patched 1 conditional null allele in mice. *Genesis*. 2003;36(3):158–161.
55. Jeong J, Mao J, Tenzen T, Kottmann AH, McMahon AP. Hedgehog signaling in the neural crest cells regulates the patterning and growth of facial primordia. *Genes Dev*. 2004;18(8):937–951.
56. Harada N, et al. Intestinal polyposis in mice with a dominant stable mutation of the beta-catenin gene. *EMBO J*. 1999;18(21):5931–5942.
57. Soriano P. Generalized lacZ expression with the ROSA26 Cre reporter strain. *Nat Genet*. 1999;21(1):70–71.
58. Metsaranta M, Toman D, De Crombrugghe B, Vuorio E. Specific hybridization probes for mouse

type I, II, III and IX collagen mRNAs. *Biochim Biophys Acta*. 1991;1089(2):241–243.
59. Takeda S, Bonnamy JP, Owen MJ, Ducy P, Karsenty G. Continuous expression of Cbfa1 in nonhypertrophic chondrocytes uncovers its ability to induce hypertrophic chondrocyte differentiation and partially rescues Cbfa1-deficient mice. *Genes Dev*. 2001;15(4):467–481.
60. Goodrich LV, Johnson RL, Milenkovic L, McMahon JA, Scott MP. Conservation of the hedgehog/patched signaling pathway from flies to mice: induction of a mouse patched gene by Hedgehog. *Genes Dev*. 1996;10(3):301–312.
61. Koziel L, Kunath M, Kelly OG, Vortkamp A. Ext1-dependent heparan sulfate regulates the range of Ihh signaling during endochondral ossification. *Dev Cell*. 2004;6(6):801–813.
62. Schaeren-Wiemers N, Gerfin-Moser A. A single protocol to detect transcripts of various types and expression levels in neural tissue and cultured cells: in situ hybridization using digoxigenin-labelled cRNA probes. *Histochemistry*. 1993;100(6):431–440.
63. Ho L, et al. Gli2 and p53 cooperate to regulate IGFBP-3- mediated chondrocyte apoptosis in the progression from benign to malignant cartilage tumors. *Cancer Cell*. 2009;16(2):126–136.
64. Gosset M, Berenbaum F, Thirion S, Jacques C. Primary culture and phenotyping of murine chondrocytes. *Nat Protoc*. 2008;3(8):1253–1260.